Proceedings World Geothermal Congress 2020+1
Reykjavik, Iceland, April - October 2021

Conceptual Model Update and Power Capacity Estimate, Hot Springs Bay Valley, Akutan, Alaska, USA

Mary MANN*, Pete STELLING**, Nicholas HINZ***, Dennis KASPEREIT*

*Geothermal Resource Group
77530 Enfield Lane Bldg E, Palm Desert CA 92211, USA
mary@geothermalresourcegroup.com
**Stelco Magma Consulting
***Geologica Geothermal Group

Keywords: Alaska, Akutan, exploration drilling, conceptual modeling, direct use, stranded resource

ABSTRACT

The initial conceptual model for the Hot Springs Bay Valley geothermal resource on Akutan Island, AK, has been revised in light of new data and interpretations. The 2012 conceptual model (Kolker et al., 2012) was based on exploration efforts beginning in 2008 and included data sets from an MT survey, fluid, gas and soil geochemistry, and data collected from two thermal gradient wells. The revised conceptual model incorporates additional geophysical data, targeted geological mapping, structural analysis, and the results from drilling and flow testing a third small-diameter well. The area of greatest geothermal potential is in the conceptualized upflow area, northwest head of the HSBV, where fluid and gas geochemistry data from fumaroles indicate a ~525°F (~275°C) reservoir. An outflow reservoir is also present, with cooler estimated reservoir temperatures (~356ºF (~180ºC)) and reduced permeability estimates than the upflow area. The revised conceptual model is largely consistent with the original, providing sufficient confidence to estimate power capacity. The extent of surface alteration in the valleys east and south of the fumaroles suggest a range of possible reservoir sizes, allowing pessimistic, preferred, and optimistic power capacity estimates for both the upflow and outflow parts of the resource.

1. INTRODUCTION

The City of Akutan has pursued development of a geothermal resource on Akutan for energy production since 2008, exploration and confirmation of the resource has progressed as possible with seasonal limitations for field work and funding agency requirements. Akutan was initially a prospective target for geothermal development as it is on the flank of an active volcano, and has surface manifestations of an active geothermal system. Continued work has confirmed that there is a geothermal resource available in the Hot Springs Bay Valley (HSBV) geothermal area.

Akutan has the opportunity to become a center of commerce and industry for the Aleutian chain, now with a harbor at the head of Akutan Bay and an airport on the adjacent Akun Island (Figure 1). The largest land based seafood processing facility in North America is also located here. With the support of the City of Akutan through the State of Alaska Renewable Energy Grant Fund and subsequently supplemented U.S. Department of Energy, the geothermal prospect area has been extensively studied, including geophysical surveys (magnetotelluric and gravity), geological mapping, geochemical studies, and drilling of three small diameter wells, two in 2010 and one in 2016. Work on the scenarios for development of the resource has also been completed, including infrastructure needed for power generation, transmission and maintenance, and financial feasibility.

The primary exploration drilling area through this work was on HSBV floor where surface manifestations of geothermal heat include hot springs and a geyser located along the northeast edge of the valley. A secondary area, generally referred to as the fumarole site, is located at approximately 1500’ elevation in the western part of the field. Though the indications of a higher temperature geothermal resource exist in this area, the higher cost of exploration, drilling, and development of this site were not justified for energy required to meet the island’s electricity demand. As a result, exploration drilling in the fumarole area has not yet been pursued.

The generalized exploration history for geothermal development since 2008:

- 2009-Initial field exploration, *development of initial conceptual model* of the field, prefeasibility study
- 2010-Drilling TG-2 and TG-4 to depths of 833’ (254m) and 1,500’ (457m), respectively, data interpretation, refinement of conceptual model of field, feasibility study
- 2012-2013-Additional field surveying for deep drilling at fumarole site (geologic mapping, geophysical surveys), conceptual model update, targeting and initiation of planning for deep drilling for resource confirmation and site development if a resource is confirmed
- October 2013-Start of -Planning for feasibility of continued exploration and development of geothermal project based at Fumarole area (design project including access roads, drilling, plant and pipelines, budgeting)
- 2014-Request for project rescoping to reevaluate the development of the Hot Springs site due to high project cost at fumarole site
- September 2014-Secure DOE funding that allows for drilling of additional thermal gradient well
- 2015-2016-Project re-scoping, well targeting, drilling and testing planning
- August-September 2016-Drilling AK-3 to a depth of 1955’ (596m)
- August 2017-Flow test AK-3
- 2018-2019 Comprehensive data assimilation and conceptual model update to the initial models developed in 2009.

Figure 1: View from helicopter coming into Akutan Bay from HSBV. Harbor development foreground, Trident fish processing plant on left middle ground, City is adjacent to plant, airport located on Akun island in distance.

2. INITIAL CONCEPTUAL MODEL

Two variations of a conceptual model of the Akutan Geothermal Resource were developed by Kolker et al. (2010) prior to any drilling, both of which describe the HSBV geothermal system as a single resource with a high temperature (>460 °F / >240 °C) upflow zone located at depth somewhere proximal to the fumaroles, and a lower-temperature outflow aquifer (~360-390°F / 180-200°C) that daylights as the hot springs in HSBV. The difference between the two endmember models is with alternative outflow pathways as either along the L-shaped path of HSBV, or along a northern trajectory around Mount Formidable from the fumaroles to the hot springs (Figure 2). These model variances on outflow were initially preferred because the flow paths followed major structural features identified or inferred from the surface maps available at the time. Subsequent data collection, analysis and integration between 2011 and 2018 was used to update and refine these models including geophysics, geology, geochemistry, drilling, core analyses, well testing, and model updates based on this work.

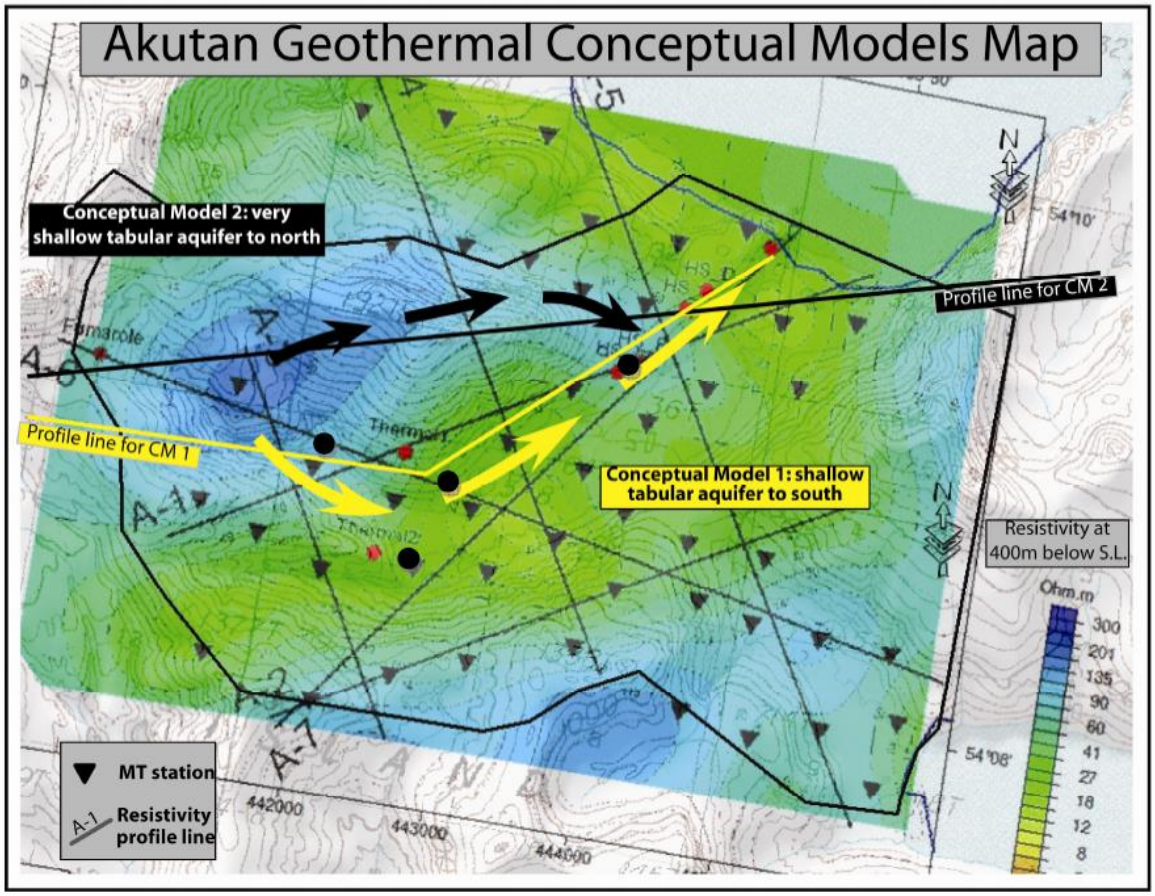

Figure 2: Map view of early conceptual model of HSBV geothermal resource showing potential flow paths from the fumarole area to the hot spring area. Shading reflects resistivity at -400 meters asl, draped over the topographic map of the area. Yellow (model 1) and black (model 2) arrows indicate the direction of shallow water outflow, respectively. Red circles indicate the location of hot springs. The upflow region is near the start of the outflow arrows just east of the fumarole field. (Kolker, et al., 2010)

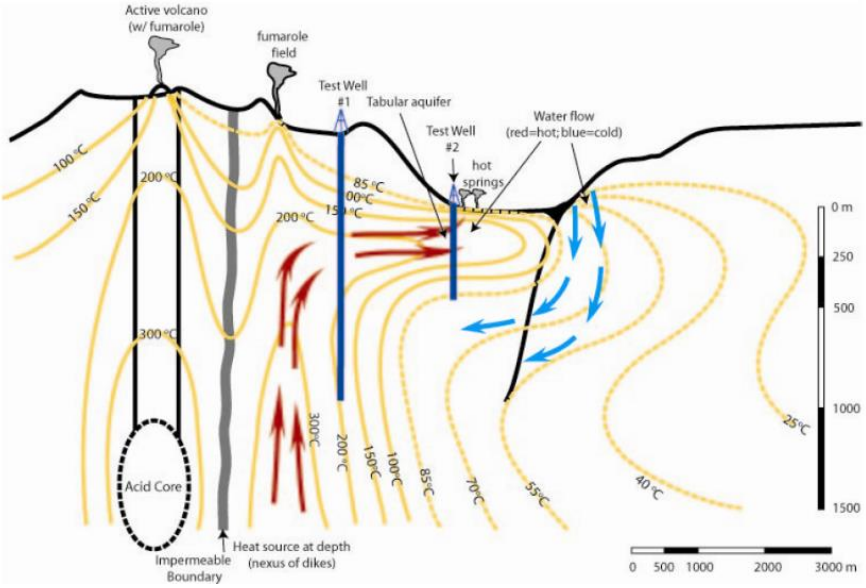

Figure 3: Cross section from the original conceptual model for HSBV geothermal resource, showing temperature patterns based on inferred flow paths affected by an intrusive heat source. In this model, shallow outflow occurs in HSBV, confined by structural features and clay aquitards. An impermeable barrier (vertical gray line) exists between the acid core of the main volcano and the geothermal system. Red arrows indicate the flow of heated water; blue arrows indicate cold water flow. (Kolker, et al., 2010)

3. EXPANDED SURFACE STUDIES – 2012

A field season in 2012 comprised the bulk of new data collection after the drilling two thermal gradient wells to contribute to the updated conceptual model. Exploration activities included:

- Expansion of Magnetotelluric (MT) survey coverage to include the inferred primary upflow area under the fumarole field.
- Collection of gravity data along with MT survey to assess variation in reservoir rocks (e.g., intrusive versus extrusive stratigraphic units) for possible joint 3D inversion.
- Conduct surface geology mapping of stratigraphy, structure, alteration and surface manifestations specifically in the prospective geothermal area.

3.1 Geology-Surface Mapping and Structural Analysis

Detailed geologic mapping and structural analyses were conducted in August 2012. Approximately 15 sq. mi. (25 km^2) were mapped, including all of HSBV, the upper half of Long Valley, and along the northeastern flank of Akutan volcano (Hinz and Dering, 2012). Key results of the new mapping include: 1) adding substantial detail to the fault mapping within the geothermal area and across the island, 2) obtaining kinematic and dip information for many of the faults, 3) completing the first detailed mapping of the alteration, 4) mapping previously undiscovered hot springs and fumaroles (Figure 4 and Figure 5).

This mapping built on existing stratigraphic studies (Motyka et al., 1991; Romick, 1993; Richter et al., 1998). The volcanic rock into which HSBV was glacially carved, consists of interbedded basaltic and andesitic lava flows, ash fall tuff layers, and breccia deposits, as observed in the valley walls as well as in the core retrieved in drilling.

Hot Springs Bay Valley was named for the several dozen hot springs present in the lower portion of the valley. The hot springs occur in a narrow (100 m wide) linear band at the base of the NW valley wall that extends ~1 mile (1.5 km) from the midpoint of the lower valley to the sea (Figure 6). Within the band, hot springs are clustered into five groups and range from 54 to 94 ^oC, with springs located further up-valley generally having higher temperatures.

At the head of the upper portion of HSBV is a vigorous fumarole field covering an area of ~85,000 sq ft (~26,000 m^2) composed of four large and dozens of smaller individual gas vents measured at 99–100 ^oC at 1,370 feet (417 m) elevation (Figure 7). The larger fumarole vents are roughly linearly aligned to the NE, as is a large boiling mud pot that appeared between 1996 and 2009 and doubled in diameter between 2010 and 2012 to ~15 m diameter (Kolker et al., 2012; Stelling, pers. Comm., 2012). There is also a lone fumarole in the drainage below the main cluster.

Faults in HSBV range from < 0.6 to 6 miles (1 to 10 km) strike length, with <65 ft (20 m) of stratigraphic offset. These structures can be classified into three groups, one striking E-W, one NE-SW, and one WNW-ESE (Figure 9). The faults are a combination of normal, oblique slip, and strike-slip motion observed across all groups. Overall, Akutan is in a transtensional tectonic setting, which is good for providing overall structurally enhanced stratigraphic permeability. However, individual faults are relatively small with little offset, and therefore have a low probability for providing major permeability zones. No major faults capable of deep circulation were observed in HSBV.

Hydrothermal alteration in HSBV consists of argillic alteration surrounding surface expression of fluid flow, especially in the fumarole area where intense alteration has created unstable ground. Significant argillic alteration exists in the bottoms of the east-west trending tributary valleys at the head of HSBV. Alteration around the hot springs is minor and limited in extent to the perimeter of each spring. Long Valley, northwest of HSBV, contains significant argillic alteration with significant silicification that is interpreted to be relict and exhumed by erosion.

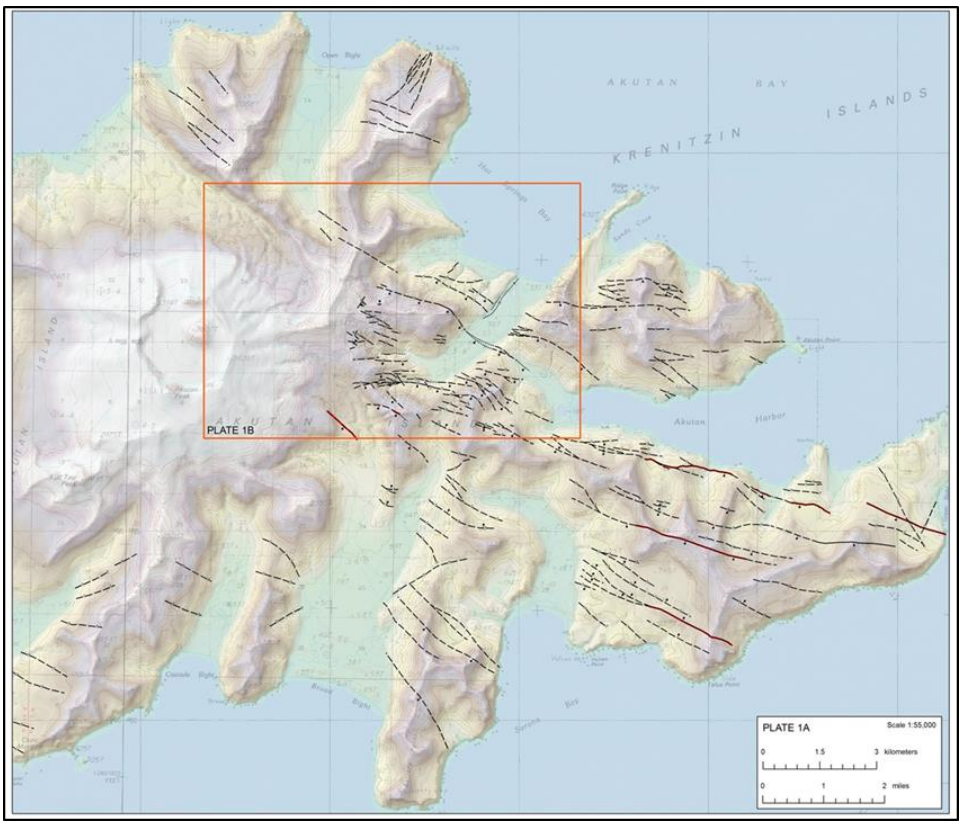

Figure 4: Fault map of Akutan Island (Hinz and Dering, 2012).

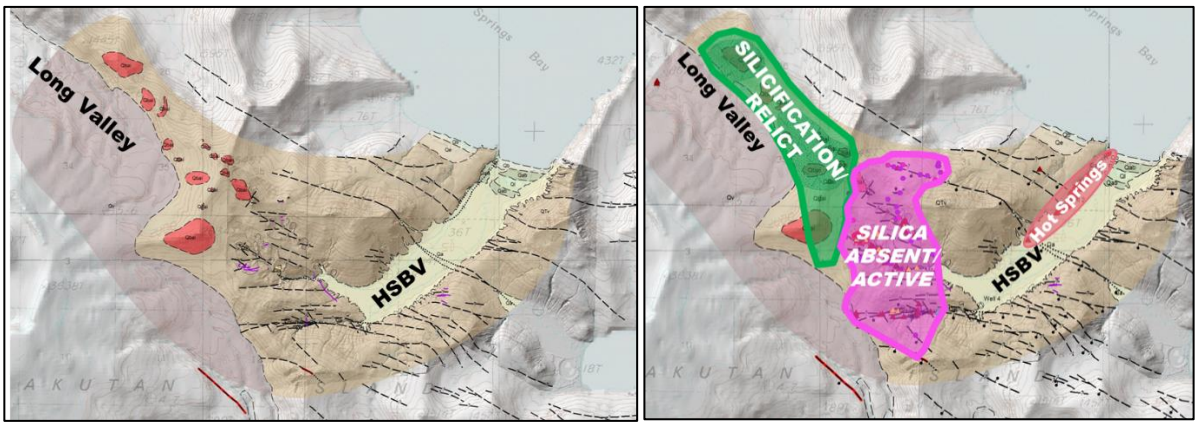

Figure 5: Geologic map of HSBV and Long Valley (Hinz and Dering, 2012) on left, compared with areas of alteration highlighted on right.

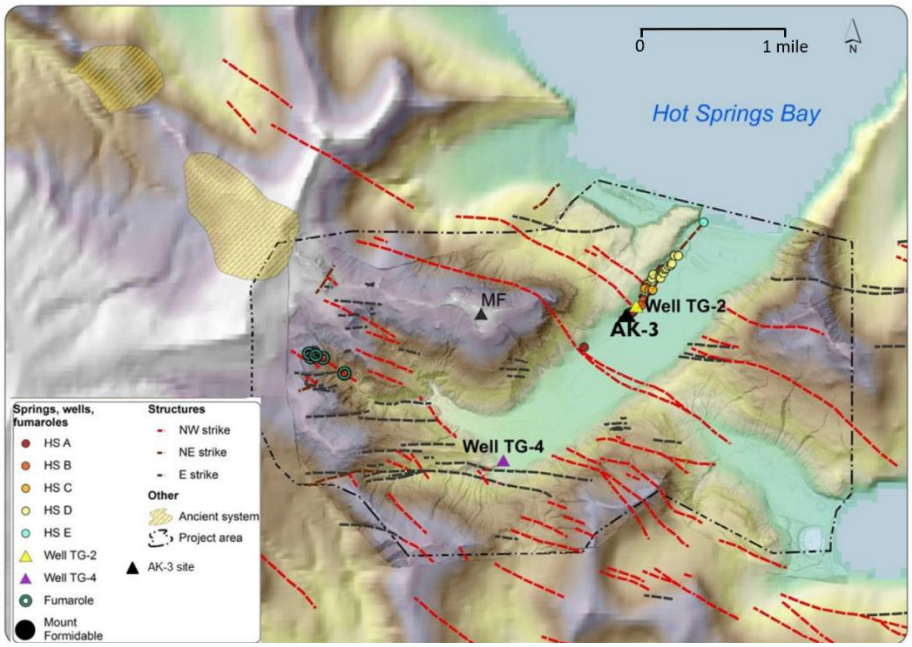

Figure 6: Distributions of geothermal surface manifestations, exploration wells within HSBV geothermal area.

Figure 7: Upper part of fumarole field viewed from north.

3.2 Magnetotelluric (MT) Survey

In 2012, a second, 46-station MT survey was conducted to complement the initial 52-station survey of 2009. The 2012 survey expanded the project area to the west to include the area west of the fumarole area and to fill in gaps. The combined data set was used to create a non-traditional 3D model by first creating 2D inversions along point to point, fence-diagrams. These were stitched together to create a 3D representation of the MT resistivity. Although this approach conveys a 3D interpretation of the subsurface resistivity, it is not 3D inversion modeling. The current model was clipped to 6,562 ft. (2000 m) below sea level to remove deeper, less reliable inversion results. Horizontal smoothing was applied to the model in order for the model to more easily predict the shallow resistivity values between widely spaced stations. Therefore, abrupt changes in shallow resistivity between stations are blurred, and steeply dipping structures (e.g., faults, or other high angle contacts between units) are not reliably resolved in the geophysical model.

Overall, the HSBV area is lacking the <10 ohm-m signatures typical of many productive geothermal systems. Although a very low resistivity (1–10 ohm-m) zone near the hot springs is present at relatively shallow depths (surface to ~150 ft. (50 m)), with higher resistivity values at greater depth, this unit is not very thick or widespread. A moderately-low resistivity unit (10–40 ohm-m) is present across most of the modeled area, particularly in the upper portion of HSBV (Figure 8). This shallow conductive layer has an average thickness of ~820 ft (250 m; maximum 1640 ft (500 m)), and forms a rough antiformal structure plunging gently to the northeast from the inferred upflow beneath the fumaroles to the outflow hot springs. The southern limb of this antiform extends to the margin of the main valley, and the northern limb thins to the NNE and is absent at the northern margin of the study area. This layer of moderately low resistivity could be the result of an immature clay cap, partial erosion of an older clay cap, or a laminated outflow interlayered with relatively high permeability (and therefore more readily altered) lithologies bracketed by lower permeability units, resulting in a higher overall resistivity signature. The drill core contains altered ash fall layers with elevated permeability

surrounded by lower permeability lava flow units, supporting the idea of a lithologically constrained outflow sheet. Additionally, mineralogical evidence from the core shows high-temperature alteration minerals present at surprisingly shallow depths, indicating there may have been significant erosion of the clay cap. However, surface exposures of alteration near the upflow are argillic, rather than propylitic, suggesting that any erosion of the clay cap has been incomplete, and some clay cap remains.

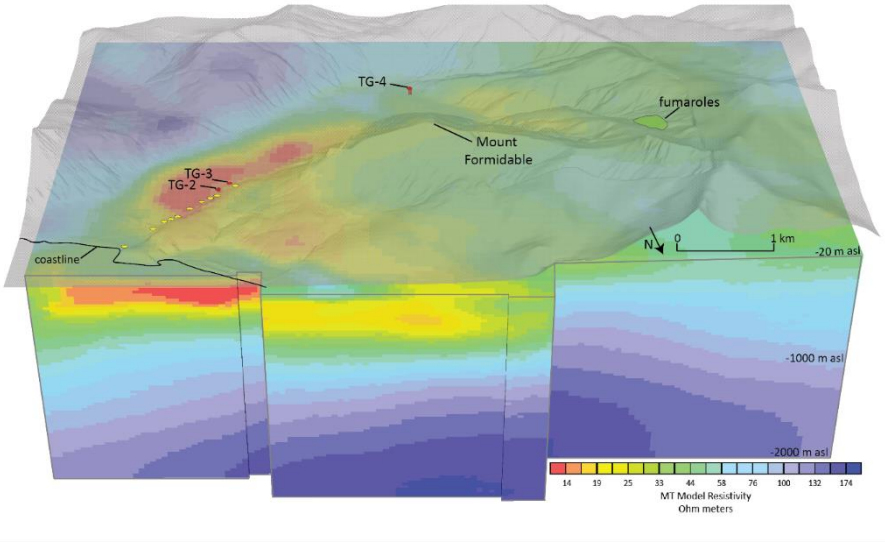

Figure 8: Integrated 2009 and 2012 MT results, view to SSW. Top surface is topography, and labels point to surface features and expressions; yellow ovals are generalized hot spring locations. The 30-40 ohm m iso-resistivity surfaces (green) extend from beneath the fumaroles beneath Mount Formidable in a general antiform structure. Lower resistivity patterns are observed along the main trend of HSB Valley and along the coastal flank of Mount Formidable. The <14 ohm-m iso-resistivity regions (red) occurs only near the hot springs and at deeper levels beneath the coastal bench. Top of MT data truncated at 20 m below sea level.

3.3 Gravity

A gravity survey was conducted in 2012, concurrent with the MT survey. A pseudo-basement surface was created from the gravity data assuming an average density of 2.33 g/cm^3. Figure 9 shows elevation contours on this pseudo- basement surface, with colors representing the MT resistivity model slice at 300 m below sea level. Although the exact values of the pseudo-basement contours depend on the assumed rock densities, the shape and gradient of the contours reveal dense elongate body that extends from the ridge southwest above HSBV to the northeast beneath Mount Formidable, suggesting higher densities in this area (Figure 9). The gravity data is consistent with MT results and surface features as well, aligning with the northwest margin of the conductive zone and the northwest valley margin (i.e., in line with the chain of hot springs in the lower HSBV). This linear expression has been interpreted to be structurally controlled.

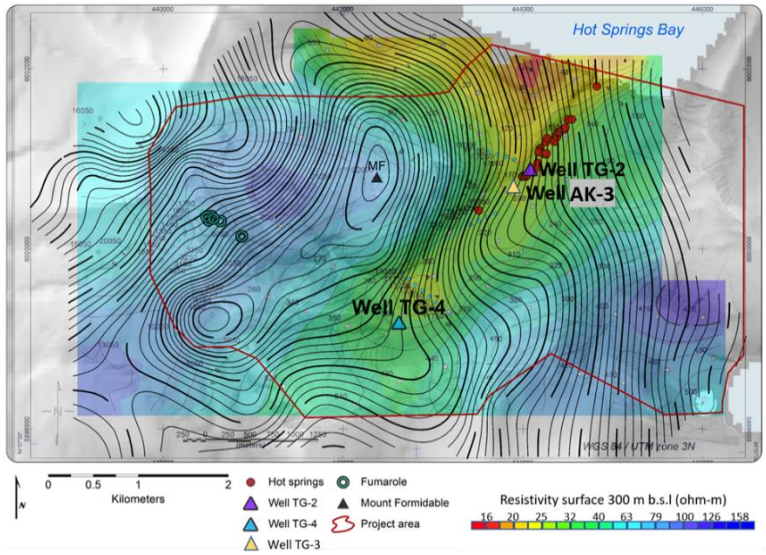

Figure 9: Map view of MT resistivity at 300 m below sea level (colored background; see legend), with gravity pseudo-basement depth contours superimposed. Gravity modeled assuming a density of 2.33 g/cm3 (contour interval 25 m, heavy contours every 100 m). Note the isolated gravity highs beneath MF and beneath the ridge south of the HSBV fumaroles. Small gray boxes are 2009 MT stations; small light blue circles are 2012 MT stations. Figure from Stelling et al., 2015.

4. GEOCHEMISTRY

Fluid and gas samples have been collected from various locations on Akutan by a variety of investigators. There are published fluid geochemical data from hot springs, meteoric water and fumarole gases (Motyka and Nye, 1988; Motyka et al., 1993; Symonds et al., 2003a, b; Bergfeld et al., 2014) and were used in the initial 2009 conceptual model and subsequent revisions. Several samples have been gathered during exploration work including water samples collected during drilling of TG-2 and TG-4 and the well test of AK-3. The chemistry indicted from work to date is that of a mature neutral-chloride reservoir brine and geothermometry indicates equilibrium temperatures above 200°C (390°F). The geothermometry temperatures have been confirmed by downhole temperature measurements in wells TG-2 and AK-3.

5. DRILLING, WELL TESTS, CORE DATA

Three exploration wells have been drilled in HSBV, the first two (TG-2 and TG-4) in 2010 and AK-3 in 2016. Well targets, well design, depth, diameter and testing options for all three were influenced and limited by the accessibility limitations into HSBV, environmental concerns with wetlands and streams, water accessibility and the significant terrain between the valley floor and the fumarole area. All three were targeted to explore the outflow part of the resource.

During drilling, TG-2 encountered high geothermal gradient with a peak in well fluid temperature between 587-583 ft (178 and 179 m) depth at a highly permeable zone that vigorously flowed 359°F (182°C) geothermal fluid. In order to drill and test deeper formations, this zone was cemented and cased off before flow-rate measurements could be conducted. Due to a host of complications during drilling, many stemming from the unexpectedly high temperature at shallow depth, TG-2 was terminated at 833 ft. (254 m), approximately half the planned total depth.

Well TG-4, located at the southwestern corner in the upper part of HSBV, was drilled to the planned 1,500 ft. (~500 m) depth. As expected of a well located just outside the margins of an outflow, no significant water flow was encountered in TG-4 and indications of high permeability were not encountered below ~213 ft (65 m).

AK-3 was selected to test as deep as possible to intersect faults that may be carrying geothermal fluids to the surface in a similar surface location to TG-2. A deeper hot resource in this lower part of the valley could be attractive for development, if viable, as compared to the shallow outflow resource that interacts too easily with the surface waters or the deeper resource inferred to exist in the fumarole area, which is less accessible. The AK-3 well was planned to be tested, unlike the first two wells, which were drilled as thermal gradient wells. In AK-3, this shallow zone encountered in TG-2 was anticipated and cased through in order to drill into a potential deeper reservoir.

5.1 Geothermal Gradients and Measured Temperatures in TG wells

The equilibrated temperature profile in TG-2 shows two zones of steep geothermal gradients in the upper half of the well: 6°F/100ft (110°C/km) from 20 to 118 ft. (6 to 36 m), and up to 25°F/100ft (460°C/km) from 118 to 400 ft. (36 to 122 m), below which temperature gradient flattens. The hottest equilibrated temperature recorded in this well is 170°C (338ºF), which occurred at 584 ft. (178 m). This temperature is 12°C (53°F) cooler than flowed water temperatures measured at this depth during drilling, suggesting that the 182°C (359°F) fluid was being "pulled in" laterally from a nearby region of limited volume. In the interval between the maximum equilibrated temperatures and total depth of 833 ft. a modest temperature reversal (~40°F; ~5°C) is present.

Steep geothermal gradients were observed at the top of TG-4, asymptotically approaching an isothermal temperature of 325ºF (163°C), suggesting that, although the well is outside the main upflow or outflow, it is being conductively heated from a nearby geothermal reservoir.

Well AK-3, located ~700 ft (~200 meters) up-valley from TG-2 encountered a fracture at 165 ft (50 m) where the well flowed, but the shallow permeability is inconsequential for the geothermal development. The well was cased to 800 ft (244 m) because, although there were permeability indicators between 700 and 800 feet, the potential deeper reservoir was the target of the third well. The hottest part of the well is at about 400 ft (122 m) depth at 357°F (180ºC), with a declining temperature profile below, indicating a hot water entry shallow, interpreted to be horizontal permeability as is found in the outflow part of the geothermal system (Figure 10). The well was able to flow only intermittently, with minimal recharge from the open hole section between 800 and 1000 ft (244 to 305 m).

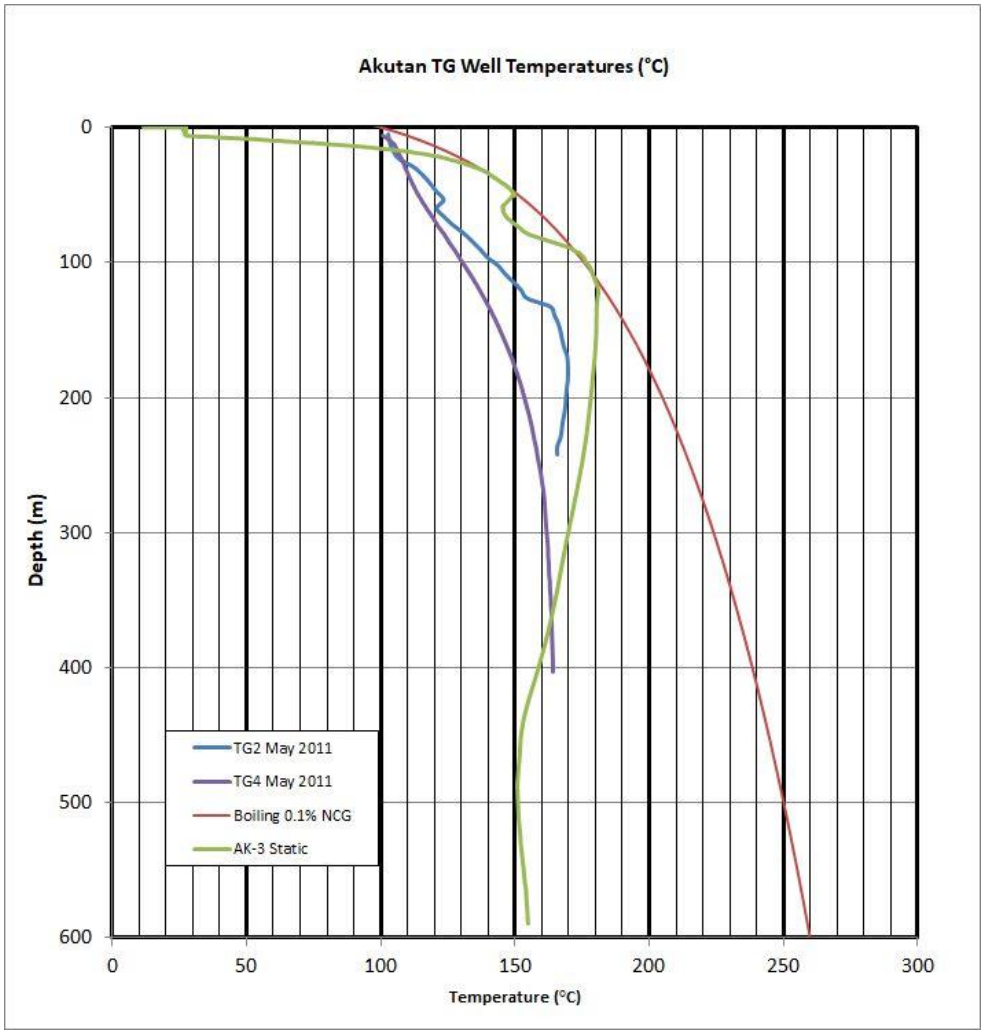

Figure 10: Temperature profiles for all three Akutan wells.

5.2 Core Data

Lithology

The stratigraphy in all three wells includes hetereolithic sequences of andesitic lavas, tuffs, and volcaniclastics with a thin layer of Late Pleistocene or Holocene surficial deposits (glacial, alluvium, landslides). Direct lithologic correlation between any of the three HSBV wells is difficult due to the lack of unique lithologies and the localized nature of many volcanic deposits.

Permeability

The matrix permeability of lithologies encountered in the HSBV wells are likely to be low. In wells TG-2 and TG-4, the permeability of lava flows is low, with tuffs and mass wasting deposits having slightly greater matrix permeability qualitative lab analyses. Secondary mineralization along clast margins in some mass wasting deposits indicates that fluid flow through this lithology has been directed around clast boundaries in the past. Higher permeability, based on the abundance and aperture of open mineralized fractures, appears to be generally restricted to the upper 900 ft. (274 m) of AK-3. In the shallow portions of TG-2 and AK-3 the fracture zones are within the mass wasting deposits. Most fractures in andesite and tuff appear to be sealed with secondary mineralization, suggesting these were fluid pathways in the past but do not appear to have significant permeability now. Alteration in shallow portions of AK-3 is very similar to that observed in TG-2, except for a narrow zone of what appears to be intense alteration along a fracture network at 168 to 170 ft. (551 to 557 m). This is likely the depth that produced the uncontrolled flow during drilling. Well TG-2 encountered a broad fracture zone at 588-590 ft. (179 to 180 m), with significant mud losses and permeability. A similar zone at this depth was not encountered in AK-3. Thus, the flow zone may only occur on one side of the fault presumed to exist between these wells.

Alteration

Alteration is dominated by moderate propylitic alteration occurring in at least two different episodes evidenced by the presence of chlorite, zeolites, epidote, prehnite, pyrite, hematite, quartz and calcite. The presence of clays is an important aspect of geothermal systems, with smectite clays helping to form a low-permeability clay cap, and high-permeability illite and chlorite clays forming regions of higher permeability. Smectite, illite and mixed-layer clays occur sporadically throughout the core, primarily along fracture margins and lithologic contacts. No thick zones of intense clay alteration were observed, although alteration is more intense in ash-fall tuff units and some volcaniclastic units. Smectite occurs at a depth of about 100 to 800 ft. (33 to 244 m), often associated with

fine-grained rocks. Illite occurs throughout the core, including at shallow depths (397 ft. (121 m) in TG-4 and 121 ft. (37 m) in TG-2). (The clay species indicated through X-ray Diffraction analysis of samples from TG-2 and TG-4.) The localized presence of kaolinite indicates advanced argillic alteration with lesser extent and lower intensity than propylitic or argillic alteration. The lack of abundant clay alteration suggests that permeability at depth in the HSBV system is less than excellent, as the circulation of hot fluids would produce more clay alteration at the top of the system. In order for a large, high-pressure geothermal system to exist under HSBV, it would need to have a fairly robust seal that includes abundant clays.

Non-clay alteration minerals in the core suggest a long history of outflow beneath the floor of HSBV. The sequence of zeolite minerals mordenite, heulandite, chabazite, laumontite, yugawaralite and wairakite indicate a pattern of increasing temperatures with depth. Epidote, clinozoisite, and chlorite are all present, consistent with fluid temperatures above ~220ºC. The occurrence of these minerals is shallower than often reported, suggesting that there may have been erosion of some portion of the top of the alteration package.

CONCEPTUAL MODEL UPDATES

The geologic mapping and expanded MT coverage from 2012 support the model of upflow beneath the fumarole area and a lithologically and structurally controlled outflow that daylights and feeds the hot springs near the mouth of HSBV. These two distinct areas have very different surface manifestations, alteration mineralogy, fluid chemistry, temperatures and permeabilities. Subsequently, these two areas are two distinct parts of a single geothermal resource for exploration and development. Conceptual models, exploration strategies, and risk factors are discussed in this section for both the upflow and outflow parts of the system.

Fumarole Resource Area

The area of greatest geothermal potential at HSBV is in the upflow zone near the fumaroles at the head of HSBV. Geochemical data from the fumaroles (Stelling et al., 2015) suggest that a deep reservoir is present that probably consists of a brine liquid capped by a small two-phase region (steam cap) with temperatures approaching 570 °F (300 °C), and producible reservoir temperatures between 482°F (250°C) and 527°F (275°C). Resistivity data suggest that the upflow reservoir is situated in brittle rocks, implying propylitic alteration regime and a good possibility of high permeability. The new mapping revealed a previously unrecognized an area of dense, overlapping, fault, fracture, and dike orientations (NE-, NW-, and E/W), another potential indicator of high permeability. The extent of surface alteration in the valleys east and south of the fumaroles suggest a range of possible reservoir sizes, which is the basis of the majority of the variation between P10, P50 and P90 resource areas (Figure 11).

Geochemistry of fumarole gases and fluids suggest that the fluids present are likely near neutral pH, an important characteristic of productive geothermal systems. Mineralogy associated with the fumaroles include smectite clays with minor kaolinite, and minor to trace native sulfur deposits. This mineral assemblage is consistent with near-neutral fluids.

Hot Springs Resource Area

The absolute path of the outflow is less constrained than the upflow, but it appears to flow broadly to the NE from the fumarole beneath Mount Formidable based on MT resistivity patterns, alteration patterns, surface expressions and measured spring temperatures. The broad MT resistivity patterns suggest this portion of the outflow is lithologically controlled, and relatively abrupt margins of resistivity patterns at the margins of the outflow suggest localized structural controls. The two flow paths suggested by Kolker et al., (2012) represent the southern and northern margins, respectively, of a more widely spread outflow (Figure 11).

The southern flow margin appears to be controlled by NW/SE structures parallel to the upper portion of HSBV and perpendicular to the main valley (Figures 11, 12). These structures extend from the fumarole field to the juncture with the main valley, where fluid flow is apparently diverted NE along structures that form the northern margin of the main HSBV. Fluids travel parallel to the valley wall until they intersect cross-valley faults that cause the fluid to ascent, forming the chain of hot springs (Figure 12).

The northern flow margin is less rigidly constrained than the southern boundary but likely involves lithologically-controlled fluid flow from the upflow toward the ENE to the north of Mount Formidable until these fluids encounter a series of NW/SE trending structures parallel to those forming the southern flow boundary at the head of the valley. Fluids are diverted to the SE to the intersection of these cross-valley faults and the valley-parallel faults of the southern flow boundary (Figure 11). Based on MT resistivity, it does not appear that the outflow is significantly deeper than 650 ft. (200 m) below sea level (up to 1000 ft. (300 m) below the surface) along the cross-valley faults (Figure 13) or that the outflow extends significantly beneath the floor of HSBV toward the center of the valley. MT low-resistivity patterns extend NE across the NW/SE trending faults, suggesting these structures are not impermeable boundaries. The extent to which these structures allow fluid flow across them is the greatest source of uncertainty in the estimates of outflow resource volume and the risk associated with development of this resource.

The intersection of the northern and southern flow boundaries (fault zones) is located near the hot springs. It is likely that the valley-parallel and cross-valley structures exhibit sufficient control over fluid flow that a portion of the outflow fluids are forced to daylight in this area (Figures 11, 12, 13). Within the margins of the outflow, however, fluid flow appears to be distributed through lithologic units. The relatively high MT resistivity signatures in this area (>10 ohm-m) may result from fluid flow and alteration within several-meter-thick permeable lithologies bracketed by relatively impermeable (i.e., unaltered) units, resulting in a high average resistivity signature. The distributed and lithologically controlled fluid flow suggests that the greatest probability of exploration success will occur where fluid flow has been concentrated (e.g., near the hot springs area). Additional wells located further up-valley on the valley floor and directly north of Mount Formidable are less likely to encounter high fluid flow rates. Wells drilled NW of the hot springs, on top of the bench that forms the NW valley wall, are more likely to encounter higher fluid flow (Figure 11).

Because much of the data suggest low permeability conditions in the outflow portion of the HSBV, producing the outflow resource entails more risk. In addition to the well behavior and alteration patterns observed in the core, there is no well-developed clay cap to indicate that a large, very permeable reservoir volume at 360- 428ºF (180-220°C) exists under HSBV. The lack of widespread surface

alteration, geochemical, and ground temperature anomalies (Kolker and Mann, 2009; Kolker et al., 2012; Stelling et al., 2015) in HSBV are consistent with this interpretation. Additionally, the chemical composition of the hot springs fluids suggests that outflow fluids become extensively mixed with cooler meteoric waters near the surface, raising concerns about cold water influx into the outflow system with production.

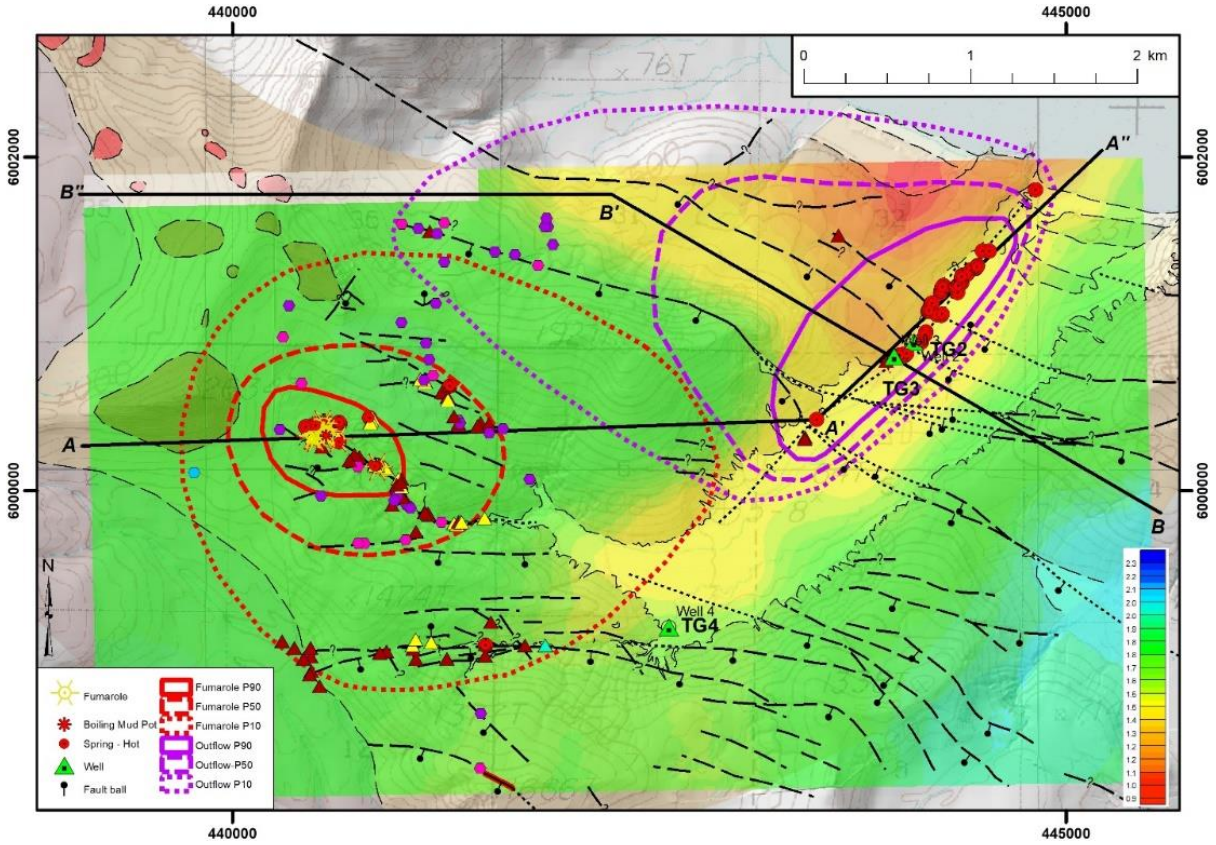

Figure 11: Map view of P90 (pessimistic; solid lines), P50 (median; dashed lines), and P10 (optimistic; dotted lines) probabilistic resource areas for fumarole and outflow parts of HSBV. Background MT resistivity slice at 100 m below sea level.

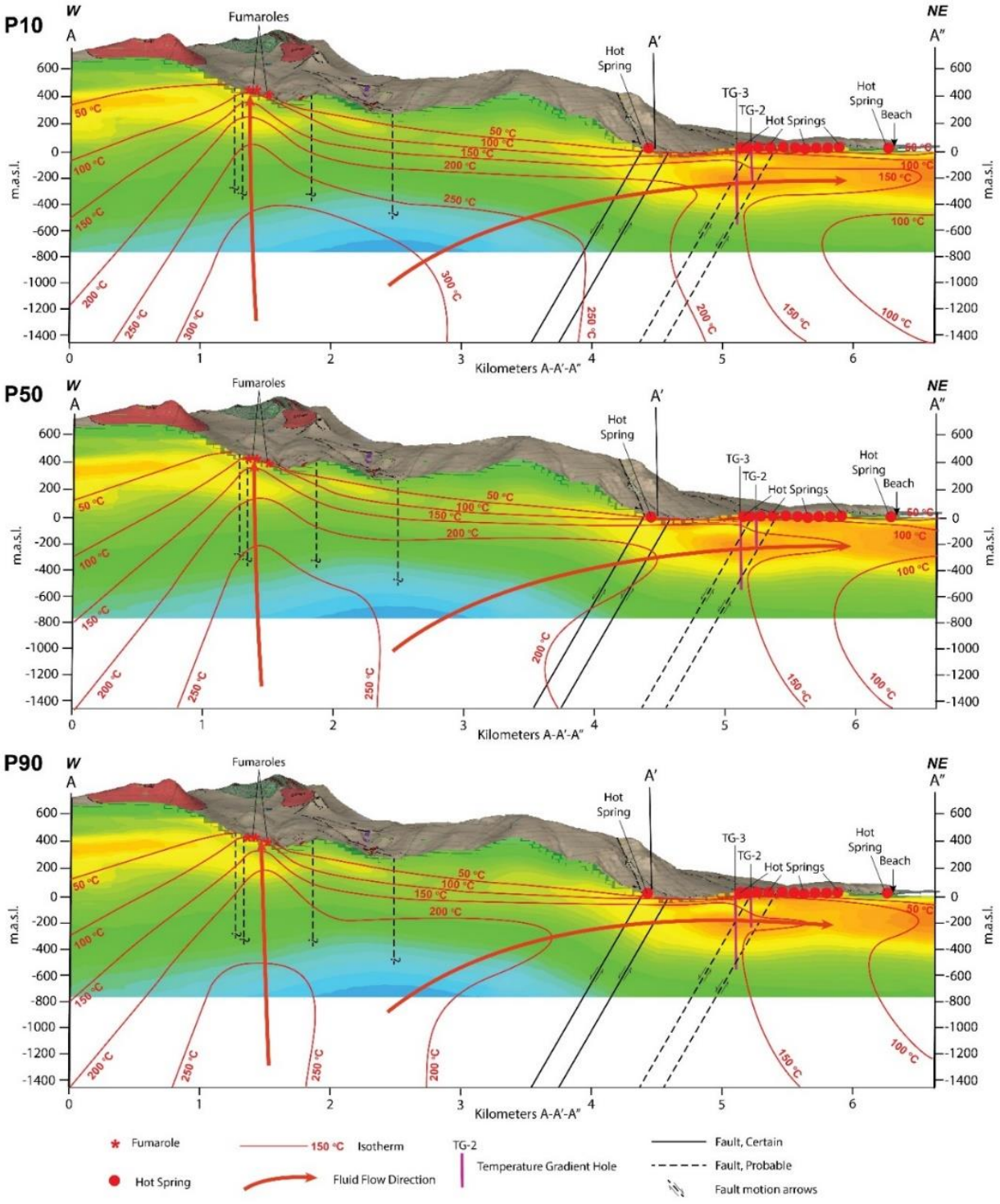

Figure 12: Valley parallel cross-sections of the P10 (optimistic; top panel), P50 (median; center), and P90 (pessimistic; bottom panel) probabilistic resource areas for fumarole and outflow resources of HSBV. Scale for MT resistivity background is the same as Figure 11.

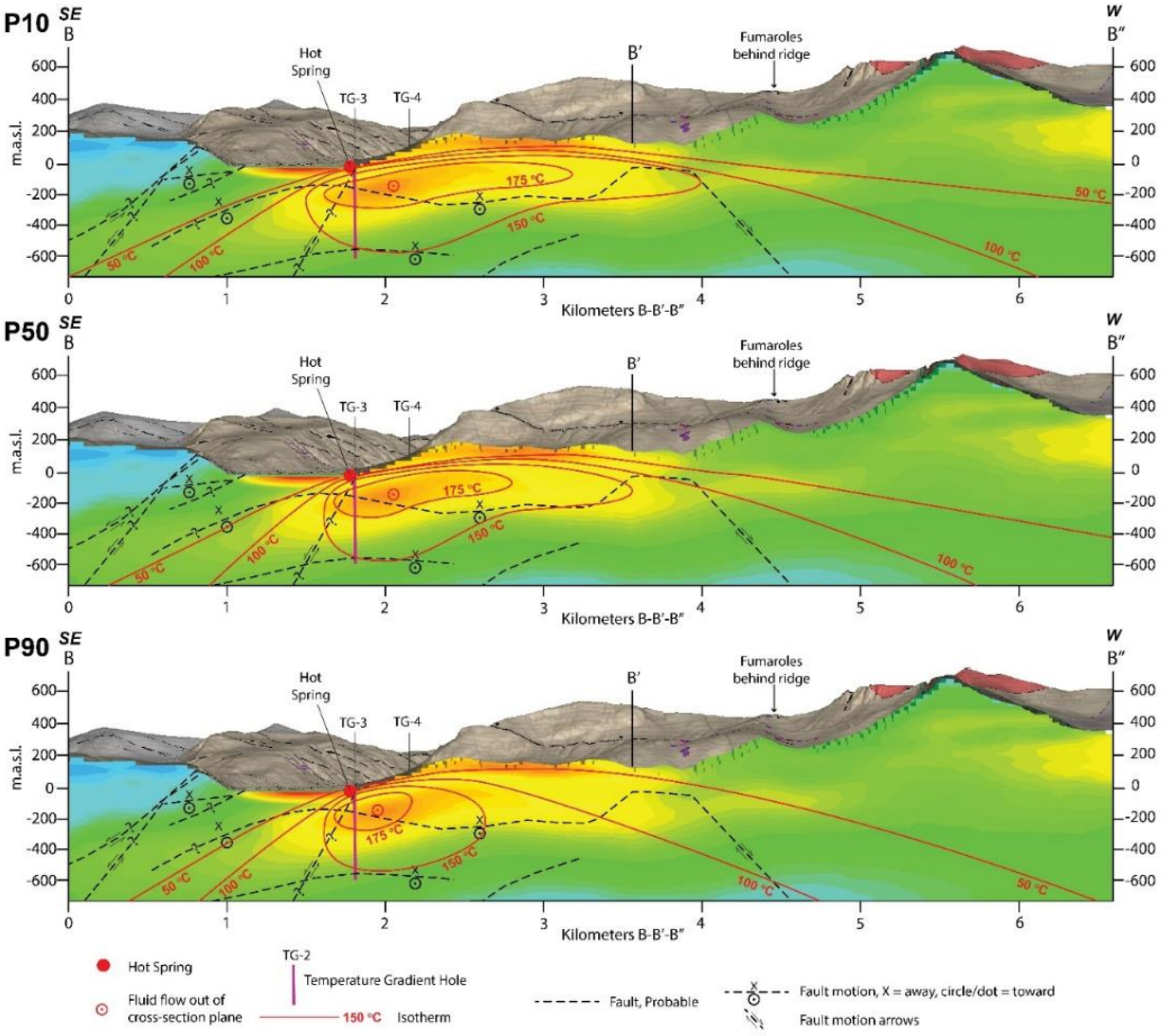

Figure 13: Valley perpendicular cross-sections, facing SW of the P10 (optimistic; top panel), P50 (median; center panel), P90 (pessimistic; lower panel), and probabilistic resource areas for fumarole and outflow resources of HSBV. Scale for MT resistivity background is the same as Figure 11.

RESOURCE CAPACITY ESTIMATION

There are a variety of ways to estimate resource capacity in geothermal systems. Heat-in-place estimates for geothermal systems are common but often overestimate resource capacity by large factors, even orders of magnitude, due to unreasonably optimistic recovery factors (Grant, 2015). Power density estimates can often be as accurate as more complex heat-in-place estimates at the exploration stage as they rely on fewer assumptions and are calibrated against a large number of known operating fields (Wilmarth and Stimac, 2015).

A power density estimate was made for two parts of the HSBV geothermal system. The intent of the power density approach is to account for the uncertainty of the resource by estimating the most optimistic values (P10, or a 10% probability that the resource is that large) and the most pessimistic values (P90, or a 90% probability that the resource is at least that large) and creating a statistical average estimate for power capacity (P50). The estimates have been made using the worksheet provided by Cumming (2016) which assumes log-normal distributions between P10 and P90. These estimates use the map area (km^2) of the reservoir size, the estimated maximum and minimum reservoir production temperatures (°C) and an assumed average power density (MW/km^2). The aerial extent of the productive resource is obtained from interpretation of the conceptual model (Figure 11, 12, and 13). The maximum and minimum temperature estimates are based on measured temperatures and fluid and gas geothermometry. The estimated power density is derived from the power densities associated with 80 operating geothermal systems worldwide (Figure 14), which provides a range of power densities based on the minimum and maximum reservoir temperatures.

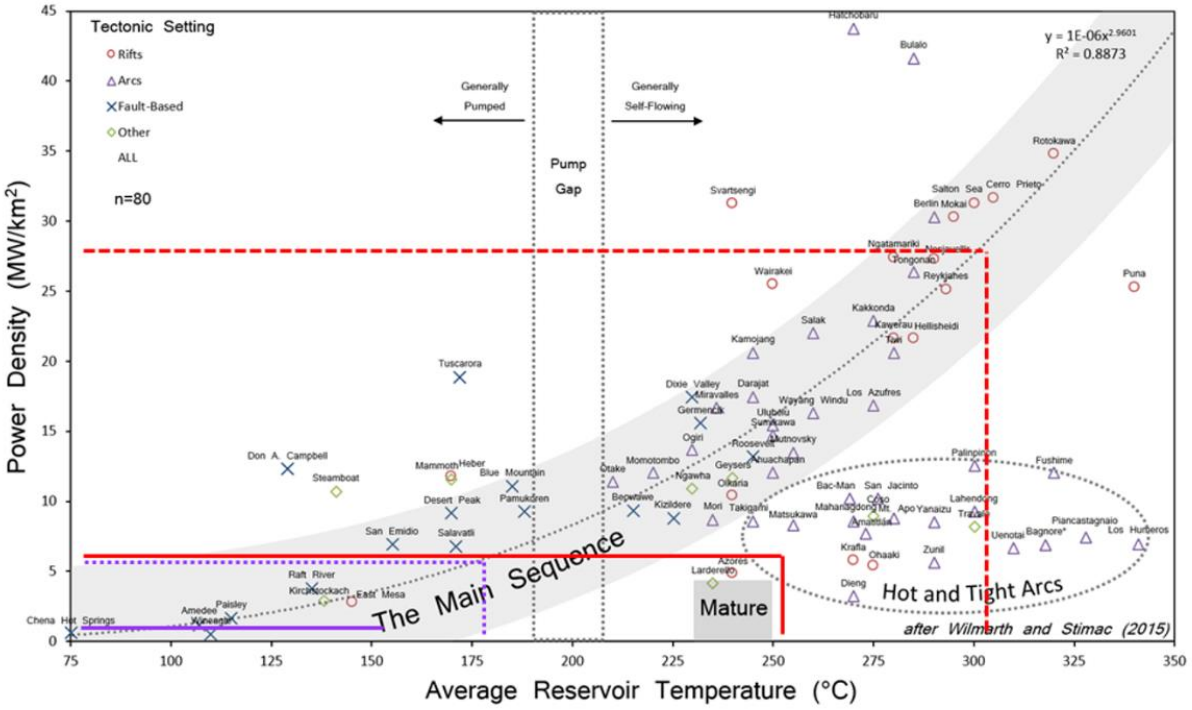

Figure 14: Power density plot of about 80 analog systems (Wilmarth et al., unpublished). Red lines correspond to temperature and power density ranges of the fumarole resource; purple lines correspond to temperature and power density ranges of the outflow resource. Dotted lines represent P10 (optimistic) values; solid lines represent P90 (pessimistic) values.

Fumarole Resource Power Capacity Estimates

The resource areas for both the fumarole and hot springs resources are based on the conceptual models developed for the upflow and outflow regions. The conceptual models incorporate all physical, chemical, and geophysical data collected to date. Based on these factors, the fumarole resource has a production area between 0.2 (pessimistic, or P90) and 3.8 (optimistic, or P10) sq. miles (0.4 and 6.4 km^2, respectively). These areas are elongate (to the SE for the upflow, SW for the outflow) due to the influence of the observed surface faults (Figure 11).

Geothermometry of the fumarole area ranges from ~250 to 275°C, possibly up to 300°C. Therefore, an estimated temperature range of 250-300°C was used. This corresponds to an expected power density range of 6-19 MW/sq. mi (10-32 MW/km^2; Figure 14). Many of volcanic systems in these temperature ranges have 3-6 MW/sq. mi (5-10 MW/km^2), but those with more favorable intra-arc tectonic setting can have greater power densities (Hinz et al., 2016). Specifically, the systems with the highest power densities in this range (Berlin, El Salvador; Mokai, New Zealand; Salton Sea, California, USA; Cerro Prieto Mexico) have a greater extensional tectonic component than is observed at Akutan. Therefore, we have reduced the most optimistic resource density estimates (P10) to systems associated with more relevant tectonic settings. This reduces the optimistic value for the fumarole power density from 32/km^2 to 27 MW/km^2. A similar approach has been made for the pessimistic (P90) power density estimate, reducing this value to 3 MW/sq. mile (5 MW/km^2), which is consistent with analogous systems Zunil (Guatemala), Amatitlan (Guatemala) and Uenota, (Japan). The wide range is justified based on the active Quaternary faulting across the island, coupled with a moderately transtensional setting.

Hot Springs Resource Power Capacity Estimates

The hot springs resource is likely composed of one or more broad lithologic units with relatively high permeability with fault systems on the SE and NE margins that constrain and consolidate fluid. The highest concentration of hot fluid is likely to be near the intersection of these fault systems, near TG-2 and AK-3. The size of the resource is largely dependent on the volume of the more permeable strata and distribution of fractures and small faults in the area that extend from the fumaroles and beneath Mount Formidable, as well as how much fluid can penetrate the NW/SE trending fault system that crosses the lower HSBV. The estimates of resource area range from 0.6 to 3.8 sq. miles (1 to 6.4 km^2; Figure 11), with a mean area (P50) of 1.5 sq. miles (2.5 km^2).

The outflow resource has geothermometry values of 356ºF (180°C) and measured temperatures of 336ºF (169°C). Thus, an estimated range of 150 to 170°C was used in the estimate. As with the fumarole resource, the estimates for power density of the hot spring resource have been reduced from 6 MW/sq. mile (10 MW/km^2) to 3 MW/sq. mile (5 MW/km^2) based on the tectonic setting of analogous systems. The P90 (pessimistic) value has been maintained at 0.6 MW/sq. mile (1 MW/km^2).

Exploration Confidence Factors

The worksheet used for estimation handicaps undiscovered resources with exploration confidence factors for the probability of discovering commercial temperature, permeability and favorable reservoir chemistry. For the fumarole resource, temperature estimates are based on fluid and gas geothermometry with no measured subsurface temperatures. Accordingly, the confidence in obtaining reservoir temperatures >250°C (P_{Temp}) has been estimated at 80%. Permeability is always the most challenging

characteristic to predict, and a $P_{Permeability}$ of 65% was chosen, typical of other undiscovered resources at this stage of exploration in similar favorable structural settings. Reservoir chemistry in the fumaroles has several indicators of being benign and consequently a $P_{Chemistry}$ of 99% was chosen. The combination of these factors results in a probability of exploration success (POS_{expl}), the chance that at least one commercial well will exist) of 51%. With this handicap, the expected mean capacity is 21 MWe and the P50 (most likely) capacity is 9 MWe (Figure 15).

EXLORATION: Is it there?

Assuming a likely exploration geoscience program and drilling program, what is the percent confidence that at least one well is commercial

	Confidence in temperature.		Confidence in permeability. Commercial mDarcy		Confidence in chemistry. Not corrosive or scaling		Probability of exploration success
	PTemperature		PPermeability		Pchemistry		POSexpl
Exploration Confidence	80%	*	65%	*	99%	=	51%

APPRAISAL AND DEVELOPMENT: Assuming it's there, how big is it?

Cumulative confidence of representative optimistic case = 10% That is, the larger, more optimistic case is assumed to be P10

Temperature range of permeable reservoir area from resource conceptual model. This should be consistent with assumed power density distribution.

Startup average production temperature for P90 reserves = 250 °C 275 °C = minimum temperature for P10 reservoir

Nu and Sigma are the mean and variance in log units required for specifying lognormal distributions in tools like @RISK

Representative Cases		P99	P90	Pessimistic P90	Middle P50	Optimistic P10	P10	P01	Mean	nu	sigma
Area > 275°C	(km^2)	0.1	0.4	0.4	1.6	6.4	6.4	19.6	2.9	0.46608	1.07867
Power Density 275 to 250 °C	(MWe/km^2)	2.5	5.0	5.0	11.6	27.0	27.0	53.7	14.4	2.45264	0.65795
MWe Capacity		1.0	3.7	3.7	18.5	93.5	93.5	350.0	41.1	2.91872	1.26350

EXPECTED POWER CAPACITY RESERVES (based on analogous reservoirs used to assess confidence in power density and area)

Expected Mean Capacity = 21 MWe = [Probability of Exploration Success] * [Mean Capacity of Development Assuming Exploration Success]

Expected P50 Capacity= 9 MWe = [Probability of Exploration Success] * [P50 Capacity of Development Assuming Exploration Success]

Adapted from Cumming, W., 2000. Spreadsheet for geothermal resource capacity scoping using lognormal area and power density distributions. Proprietary course material.

Figure 15: Power capacity calculation for the fumarole resource.

The probability of exploration success for the outflow resource is similar to that of the upflow. Measured temperatures are consistent with geothermometry results, allowing a P_{Temp} of 100%. Measured fluid chemistry is benign, allowing a Pchem of 95%. Production-grade permeability is a larger concern in the outflow, as drilling and testing results to date have not confirmed sustainable commercial flow rates. Thus, a P_{Perm} of 45% was chosen. This yields a POS_{expl} of 43%. Thus, the mean power capacity of the outflow resource is 3 MWe and the P50 (most likely) power capacity is 2 MWe (Figure 16).

EXLORATION: Is it there?

Assuming a likely exploration geoscience program and drilling program, what is the percent confidence that at least one well is commercial

	Confidence in temperature.		Confidence in permeability. Commercial mDarcy		Confidence in chemistry. Not corrosive or scaling		Probability of exploration success
	PTemperature		PPermeability		Pchemistry		POSexpl
Exploration Confidence	100%	*	45%	*	95%	=	43%

APPRAISAL AND DEVELOPMENT: Assuming it's there, how big is it?

Cumulative confidence of representative optimistic case = 10% That is, the larger, more optimistic case is assumed to be P10

Temperature range of permeable reservoir area from resource conceptual model. This should be consistent with assumed power density distribution.

Startup average production temperature for P90 reserves = 150 °C 170 °C = minimum temperature for P10 reservoir

Nu and Sigma are the mean and variance in log units required for specifying lognormal distributions in tools like @RISK

Representative Cases		P99	P90	Pessimistic P90	Middle P50	Optimistic P10	P10	P01	Mean	nu	sigma
Area > 170°C	(km^2)	0.5	1.0	1.0	2.5	6.4	6.4	13.6	3.3	0.92815	0.72424
Power Density 170 to 150 °C	(MWe/km^2)	0.5	1.0	1.0	2.2	5.0	5.0	9.6	2.7	0.80472	0.62793
MWe Capacity		0.6	1.7	1.7	5.7	19.3	19.3	52.6	9.0	1.73287	0.95855

EXPECTED POWER CAPACITY RESERVES (based on analogous reservoirs used to assess confidence in power density and area)

Expected Mean Capacity = 3 MWe = [Probability of Exploration Success] * [Mean Capacity of Development Assuming Exploration Success]

Expected P50 Capacity= 2 MWe = [Probability of Exploration Success] * [P50 Capacity of Development Assuming Exploration Success]

Adapted from Cumming, W., 2000. Spreadsheet for geothermal resource capacity scoping using lognormal area and power density distributions. Proprietary course material.

Figure 16: Power capacity calculation for the outflow resource.

CONCLUSIONS

The resource model developed through the exploration process, predicts that there is a viable geothermal resource in two general areas: on the northwest edge of Hot Springs Bay Valley going northwest of the valley (hot springs area) and southwest of the Valley (fumarole area). The resource temperature for the valley area is expected to be about 170°C (340°F) and given the size and

permeability estimates (with a factor for the level of confidence in the estimates), the mean power capacity of the outflow resource is 3-4 MWe and the P50 (most likely) power capacity is 2 MWe. The fumarole area has an expected resource temperature of >240°C (464°F) and given the size and permeability estimates mean capacity is 21 MWe and the P50 (most likely) capacity is 9 MWe. The greatest probability of overall MWe production is in the fumarole regions, but this region is hampered by accessibility. Permeability is the most difficult factor to predict, but has a significant impact on the available geothermal fluids and therefore the amount of power that can be generated. The uncertainty in this value is the main reason for lower confidence in the likelihood of exploration success and the wide range in predicted MW values.

Acknowledgements: Thank you to the City of Akutan mayor, staff, and residents for support of this work. This conceptual model update has benefited from numerous discussions with Bill Cumming.

REFERENCES

Bergfeld, D., Lewicki, J.L., Evans, W.C., Hunt, A.G., Revesz, K. and Huebner, M: Geochemical Investigation of the Hydrothermal System on Akutan Island, Alaska, July 2012. U.S. Geol. Surv. Sci. Invest. Rep. 2013-5231, 20 p. http://dx.doi.org/10.3133/sir20135231. (2014)

Cumming, W.: Resource Conceptual Models of Volcano-Hosted Geothermal Reservoirs for Exploration Well Targeting and Resource Capacity Assessment: Construction, Pitfalls and Challenges, GRC Transactions, Vol. 40, 16pp. (2016)

Geothermal Resource Group: Preliminary Summary of Findings Akutan Geophysical and Geological Investigation, For the Purpose of Delineating and Targeting the Geothermal Resource of Hot Springs Bay Valley, Commissioned by City of Akutan, Alaska (2014).

Geothermal Resource Group:, Akutan Well AK-3 Drilling Site Selection Document, Prepared for City of Akutan, 14p. (2014)

Geothermal Resource Group: Akutan Geothermal Project AK-3 End of Well Report, 29 pp. (2016)

Geothermal Resource Group: Akutan Geothermal Project, Well AK-3 Flow Test Report, August 2017, 30 pp. (2017)

Grant (2015) Resource Assessment, a Review, with Reference to the Australian Code. Proceedings WGC.

Kolker, A., P. Stelling, B. Cumming, A. Prakash, and C. Kleinholt: Akutan Geothermal Project: Report on 2009 Exploration Activities. Unpublished report to the City of Akutan and the Alaska Energy Authority, 37p. (2009)

Kolker, A., B. Cumming, and P. Stelling: Akutan Geothermal Project: Preliminary Technical Feasibility Report. Unpublished report to the City of Akutan and the Alaska Energy Authority, 31p. (2010)

Kolker, A. Cumming, W., Stelling, P., Rohrs, D.:Akutan Geothermal Resource Assessment, Commissioned by City of Akutan, 34p. (2011)

Kolker, A., Stelling, P., Cumming, W., & Rohrs, D.: Exploration of the Akutan geothermal resource area. In Proceedings, Thirty-Seventh Workshop on Geothermal Reservoir Engineering (Vol. 37). (2012)

Kolker, A., B. Cumming, and P. Stelling: Geothermal Exploration at Akutan, Alaska: Favorable Indications for a High-Enthalpy Hydrothermal Resource Near a Remote Market. Geothermal Resource Council Transactions No. 34, 14p. (2010)

Hinz, N.H. and G. Dering: "Stratigraphic and Structural Controls of the Hot Springs Bay Valley Geothermal System, Akutan Island, Alaska.", University of Nevada, Reno, Final Report, 28 pages. (2012)

Lu, Z., Wicks, C., Dzurisin, D., Thatcher, W. and Power, J.: Ground Deformation Associated with the March 1996 Earthquake swarm at Akutan Volcano, Revealed by Satellite Radar Interferometry. Journal of Geophysical Research, v. 105, No. B9, p. 21483-21495. (2000)

Mira Geoscience: Rock Density and Gravity Data Analysis, 3D Geoscience Data Integration, and Interpretation at the Akutan Island Geothermal Project, Geothermal Resource Group, Inc., Project #4309, 37 pp. (2014)

Motyka, R., and Nye, C.: A geological, geochemical, and geophysical survey of the geothermal resources at Hot Springs Bay Valley, Akutan Island, Alaska. Alaska Division of Geological and Geophysical Surveys, Report of Investigations 88-3. (1988)

Ohren, M., A. Bailey, N. Hinz, G. Oppliger, J. Hernandez, W. Rickard, and G. Dering: "Akutan Geothermal Area Exploration Results and Pre-Drilling Resource Model." Transactions of the Geothermal Resources Council, vol. 37, p. 301-307. (2013)

Powell, T., and W. Cumming: Spreadsheets for Water and Geothermal Gas Chemistry. Proceedings of the Thirty-Fifth Workshop on Geothermal Reservoir Engineering, Stanford University, Stanford, California, SGP-TR-188. (2010)

RMA Consulting Group: Phase III Progress Report, for the Period 1 September 2013 – 28 February 2014, Akutan Geothermal Development Project, Alaska Energy Authority, Grant Agreement Number 7040050 (2014)

Stelling, P. and T. Kent: "Geological Analysis of Drill Core from Geothermal Gradient Wells HSB2 and HSB4." Consultant report, Stelco Magma Consulting and Western Washington University, 24 pages. (2011)

Stelling, P., Kolker, A., and Cumming, W.: Geoscientific Data Types used to Support Geothermal Exploration at Akutan, Alaska: An Analysis of Relative Effectiveness in Thermal Gradient Well Targeting. Abstract V23D-07 presented at 2010 Fall meeting, AGU, San Francisco, Calif., 13-17 Dec. (2010)

Stelling, P., N.H. Hinz, A. Kolker, and M. Ohren: "Exploration of the Hot Springs Bay Valley (HSBV) geothermal resource area, Akutan, Alaska." Geothermics, vol. 57, p. 127-144. (2015)

Wilmarth, M. and Stimac, J, Worldwide Power Density Review, 39th Workshop on Geothermal Reservoir Engineering, SGP-TR-202, 5 pp. (2014)